BioMetals 1994, 7, 185–192

Biodistributions of radioactive bipositive metal ions in tumor-bearing animals

Atsushi Ando & Itsuko Ando

School of Allied Medical Professions, Kanazawa University, Kanazawa 920, Japan

Received 17 August 1993; accepted for publication 15 September 1993

Distributions of the nuclides $^{65}ZnCl_2$, $^{85}SrCl_2$, $^{58}CoCl_2$ and $^{103}PdCl_2$ in tumor-bearing animals were determined, and, in addition, the distributions of these nuclides in tumor tissues were observed. Their subcellular distribution in tumor and liver was also examined. Generally speaking, retention values of these bipositive metal ions in tumor were smaller than those of tri-, quadri- and pentavalent metal ions. In the case of $^{85}SrCl_2$, a large amount of this nuclide was taken up by the bone and remained there for a long time. In the case of $^{103}PdCl_2$, ^{103}Pd was avidly taken up by the kidney and liver. Very little of the ^{103}Pd taken up into the kidney and liver was excreted. ^{65}Zn and ^{103}Pd were concentrated in the viable tumor tissue and were not seen in necrotic tumor tissue. In the case of ^{58}Co, lysosome played an important role in liver accumulation and played a minor role in tumor accumulation. The distribution of ^{58}Co in tumor and liver was fairly similar to that of ^{67}Ga, ^{111}In, ^{169}Yb, ^{46}Sc, ^{51}Cr, ^{95}Zr, ^{181}Hf, ^{95}Nb and ^{182}Ta which were reported previously. Lysosome did not play an important role in the accumulation of ^{65}Zn, ^{85}Sr and ^{103}Pd into tumor and liver.

Keywords: biodistribution, bipositive metal ions, tumor-bearing animal

Introduction

Many investigations about radioactive metal compounds have been carried out to clarify the biological characteristics of radioactive metal ions. We had also been investigating the behavior of radioactive metal ions in animals to offer data which contribute to development of radiopharmaceuticals and to health physics and hygiene. To date the biodistributions of ^{201}Tl (Ando *et al.* 1987a), alkaline metals (Ando *et al.* 1988), ^{67}Ga (Ando *et al.* 1985), ^{111}In, ^{169}Yb (Ando *et al.* 1982), ^{167}Tm (Ando *et al.* 1983), ^{46}Sc, ^{51}Cr (Ando *et al.* 1987b), ^{95}Zr, ^{181}Hf (Ando & Ando 1986), ^{95}Nb and ^{182}Ta (Ando & Ando 1990) in tumor-bearing animals and mechanisms for accumulation in tumor and liver have been investigated by us. The cations of these nuclides were positive monovalent ($^{201}Tl^+$, $^{22}Na^+$, $^{42}K^+$, $^{86}Rb^+$, $^{134}Cs^+$), trivalent ($^{67}Ga^{3+}$, $^{111}In^{3+}$, $^{169}Yb^{3+}$, $^{167}Tm^{3+}$, $^{46}Sc^{3+}$, $^{51}Cr^{3+}$), quadrivalent ($^{95}Zr^{4+}$, $^{181}Hf^{4+}$) and pentavalent ($^{95}Nb^{5+}$ and $^{182}Ta^{5+}$).

Many bipositive metal ions are contained among essential metal ions. The present study was undertaken to determine the biodistributions of bipositive-metal ions containing essential metal ions and to elucidate the accumulation mechanism into tumor and liver.

Address for correspondence: A. Ando, School of Allied Medical Professions, Kanazawa University 5-11-80, Kodatsuno, Kanazawa 920, Japan. Tel: (+81) 762 222 211. Fax: (+81) 762 615 281.

Materials and methods

Materials

The following animals and transplanted tumors were used. Male Donryu rats (body weight 217.6 ± 25.2 g) underwent subcutaneous implantation of Yoshida sarcoma (1×10^8 cells per 0.25 ml) or hepatoma AH109A (1×10^8 cells per 0.25 ml) in the right thigh. 6–7 days later an appropriate amount of radioactive nuclide was administered, at which time the tumor grew to 1.5–2.0 cm in diameter. Male ddY mice (body weight 40.6 ± 4.4 g) received subcutaneous transplantations of Ehrlich tumor (5×10^7 cells/0.1 ml) in the right thigh. At 7–10 days later these mice were used in experiments, at which time the tumor had grown to about 1 cm in diameter.

$^{65}ZnCl_2$ solution (1 ml containing 0.4 MBq of carrier free ^{65}Zn) was prepared from $^{65}ZnCl_2$ in 0.5 M HCl solution (New England Nuclear, Boston, MA) and 0.9% NaCl solution.

$^{85}SrCl_2$ solution (1 ml containing 0.8 MBq and 5 μg of ^{85}Sr) was prepared from $^{85}SrCl_2$ in 0.5 M HCl solution (New England Nuclear) and 0.9% NaCl solution.

$^{58}CoCl_2$ solution (1 ml containing 0.4 MBq of carrier free ^{58}Co) was prepared from $^{58}CoCl_2$ in 0.1 M HCl solution (The Radiochemical Centre, Amersham, UK) and 0.9% NaCl solution.

$^{103}PdCl_2$ solution (1 ml containing 0.4 MBq of carrier free ^{103}Pd) was prepared from $^{103}PdCl_2$ in 1 M HCl solution (The Radiochemical Centre) and 0.9% NaCl solution.

Methods

Distribution in tumor-bearing animals. Each preparation (0.4 ml) of radioactive metal compound solutions was injected intravenously through the tail vein of the rats implanted with Yoshida sarcoma. At 3, 24 and 48 h after the administration of these nuclides, the animals were killed under sodium pentobarbital anesthesia and blood samples of about 1 ml were collected from the carotid arteries. After this, the tumor tissue, liver, kidney, spleen, parietal bone, etc. (Table 1), were excised. These tissues and the blood were weighed and counted using a well-type scintillation counter (Aloka, JDC-701) against an appropriate standard to obtain the percentage of injected dose per gram of tissue (% dose g^{-1}). This value was normalized to a body weight (BW) of 100 g by multiplying by BW/100. Furthermore, cumulative urinary excretion (0–3 h) was assayed.

Subcellular distribution in tumor and liver. Each preparation was injected intravenously into the tumor-bearing rats and intraperitoneally into the Ehrlich tumor-bearing mice. At 10 min, and 1, 3, 24 and 48 h after administration of these nuclides, these animals were killed under sodium pentobarbital anesthesia, and the tumor tissues and liver were excised. These tissues were homogenized in cold (5 °C) 0.25 M sucrose containing 0.01 M Tris–HCl buffer, pH 7.6 (10% w/v) in a Potter–Elvehjem type homogenizer. According to the modified method (Hogeboom 1955) of Hogeboom and Schneider, subcellular fractionation was carried out at 4 °C. Fractions from the centrifugation were assayed for radioactivity using the above scintillation counter.

Distribution in tumor tissue. Each preparation was injected intravenously into the rats implanted with Yoshida sarcoma and intraperitoneally into the mice implanted with Ehrlich tumor. The animals were killed under anesthesia and tumor tissues were excised at 3, 24 and 48 h after administration of these nuclides. The tissues were frozen immediately after excision in *n*-hexane (−70 °C) cooled with dry ice–acetone. Autoradiograms and sections stained with hematoxylin–eosin were prepared according to the method previously described (Ando *et al.* 1984).

Results

Distribution in tumor-bearing animals

Results are shown in Table 1. Concerning the rats administered with $^{65}ZnCl_2$, retention values of this nuclide for tumors at 3, 24 and 48 h after the administration were 0.63, 1.06 and 1.25% dose g^{-1}, respectively. These values increased with time after administration. The values for liver, spleen, kidney, pancreas and adrenal gland at 3 h after the injection were 7.12, 3.02, 3.92, 4.27 and 2.51% dose g^{-1}, respectively. However, these values decreased with time. The values for skeletal muscle, lung, cardiac muscle, brain, thymus and bone at 3 h after the injection were smaller than those for the above five organs, but increased with time. The value for blood at 3 h after injection was 0.33% dose g^{-1} and this value showed little change with time after administration. Cumulative urinary excretion rate (0–3 h) of ^{65}Zn was 0.04 ± 0.02%.

Concerning the rats administered with $^{85}SrCl_2$, retention values of ^{85}Sr for tumors were very small and decreased with time after administration. The values for bone at 3, 24 and 48 h after injection were 11.5, 11.7 and 11.8% dose g^{-1}, respectively. These values were very much larger than those for other organs. The values for blood and soft tissues were very small, and these values decreased with time. Cumulative urinary excretion rate (0–3 h) of ^{85}Sr was 4.98 ± 1.13%.

Concerning the rats administered with $^{58}CoCl_2$, retention values of ^{58}Co for tumors at 3 h after administration was 0.71% dose g^{-1}, and this value decreased with time. The values for liver and kidney at 3 h after the injection were 5.74 and 2.79% dose g^{-1}, respectively, but these values decreased with time. The values for other organs were small and decreased with time. Cumulative urinary excretion rate (0–3 h) of ^{58}Co was 29.3 ± 7.4%.

Concerning the rats injected with $^{103}PdCl_2$, retention values of ^{103}Pd for tumors were small and these values slightly decreased with time. The value for kidney was extremely large and was little changed with time. The value for liver was very large and decreased slightly with time. The values for lung, adrenal gland and spleen at 3 h after administration were 8.91, 2.48 and 4.34% dose g^{-1}, respectively. The values for lung and adrenal gland decreased markedly with time, and the values for spleen showed little change. The values for other organs were small and also showed little change with time. The values for blood were small and markedly decreased with time. The cumulative urinary excretion rate (0–3 h) of ^{103}Pd was 6.35 ± 0.52%.

Table 1. Mean retention values (% dose g^{-1}) of radioactive bipositive metal ions in tissues of Yoshida sarcoma-bearing rats at various time intervals after administration

	$^{65}ZnCl_2$			$^{85}SrCl_2$			$^{58}CoCl_2$			$^{103}PdCl_2$		
	3 h	24 h	48 h	3 h	24 h	48 h	3 h	24 h	48 h	3 h	24 h	48 h
Blood	0.33 ± 0.06	0.31 ± 0.03	0.30 ± 0.04	0.24 ± 0.02	0.03 ± 0.002	0.02 ± 0.005	0.26 ± 0.06	0.07 ± 0.01	0.04 ± 0.003	0.35 ± 0.07	0.05 ± 0.006	0.04 ± 0.001
Skeletal muscle	0.28 ± 0.04	0.36 ± 0.04	0.46 ± 0.01	0.13 ± 0.01	0.02 ± 0.001	0.01 ± 0.001	0.09 ± 0.02	0.03 ± 0.002	0.03 ± 0.002	0.08 ± 0.003	0.08 ± 0.002	0.09 ± 0.003
Liver	7.12 ± 1.25	3.48 ± 0.22	2.91 ± 0.47	0.09 ± 0.01	0.01 ± 0.002	0.01 ± 0.001	5.74 ± 0.47	2.55 ± 0.45	2.00 ± 0.09	14.1 ± 2.4	9.94 ± 1.33	9.91 ± 1.20
Spleen	3.02 ± 0.25	2.61 ± 0.26	1.88 ± 0.02	0.09 ± 0.02	0.01 ± 0.001	0.01 ± 0.001	0.44 ± 0.06	0.20 ± 0.06	0.11 ± 0.02	4.34 ± 0.93	4.00 ± 0.78	4.38 ± 0.19
Kidney	3.92 ± 0.78	2.56 ± 0.27	1.80 ± 0.31	0.28 ± 0.05	0.02 ± 0.005	0.02 ± 0.004	2.79 ± 0.38	1.08 ± 0.12	0.88 ± 0.15	20.2 ± 3.22	21.1 ± 3.01	21.4 ± 2.47
Lung	1.10 ± 0.17	1.50 ± 0.15	1.60 ± 0.31	0.23 ± 0.03	0.03 ± 0.003	0.02 ± 0.004	0.75 ± 0.21	0.27 ± 0.06	0.11 ± 0.01	8.91 ± 1.44	2.19 ± 0.28	1.80 ± 0.47
Pancreas	4.27 ± 0.80	1.78 ± 0.28	1.27 ± 0.06	0.21 ± 0.02	0.02 ± 0.002	0.02 ± 0.002	1.30 ± 0.22	0.40 ± 0.09	0.28 ± 0.08	0.38 ± 0.09	0.37 ± 0.03	0.35 ± 0.06
Adrenal	2.51 ± 0.09	1.54 ± 0.28	1.07 ± 0.08	0.17 ± 0.04	0.02 ± 0.008	0.02 ± 0.005	1.13 ± 0.13	0.76 ± 0.14	0.61 ± 0.06	2.48 ± 0.56	1.61 ± 0.17	1.06 ± 0.24
Cardiac muscle	1.19 ± 0.14	1.26 ± 0.34	1.32 ± 0.14	0.10 ± 0.01	0.01 ± 0.002	0.01 ± 0.002	0.53 ± 0.09	0.27 ± 0.01	0.25 ± 0.09	0.27 ± 0.04	0.26 ± 0.03	0.24 ± 0.07
Brain	0.16 ± 0.01	0.27 ± 0.02	0.33 ± 0.02	0.06 ± 0.003	0.02 ± 0.002	0.01 ± 0.002	0.04 ± 0.005	0.03 ± 0.005	0.03 ± 0.001	0.03 ± 0.006	0.03 ± 0.004	0.04 ± 0.001
Thymus	0.94 ± 0.15	1.51 ± 0.21	1.55 ± 0.20	0.07 ± 0.01	0.01 ± 0.001	0.01 ± 0.001	0.23 ± 0.02	0.08 ± 0.02	0.05 ± 0.02	0.28 ± 0.08	0.27 ± 0.05	0.24 ± 0.01
Bone	0.59 ± 0.17	0.84 ± 0.21	1.12 ± 0.26	11.5 ± 1.5	11.7 ± 1.2	11.8 ± 1.2	0.24 ± 0.04	0.12 ± 0.02	0.09 ± 0.02	0.17 ± 0.03	0.19 ± 0.03	0.14 ± 0.04
Tumor	0.63 ± 0.08	1.06 ± 0.29	1.25 ± 0.19	0.36 ± 0.06	0.08 ± 0.03	0.08 ± 0.04	0.71 ± 0.13	0.39 ± 0.03	0.20 ± 0.03	0.25 ± 0.06	0.22 ± 0.07	0.20 ± 0.04

Retention values in various tissues are expressed as percent of administered dose per gram tissue weight. Tissues are normalized to a body weight (BW) of 100 g by multiplying by BW/100. Each value represents the mean ± SD of data from five animals.

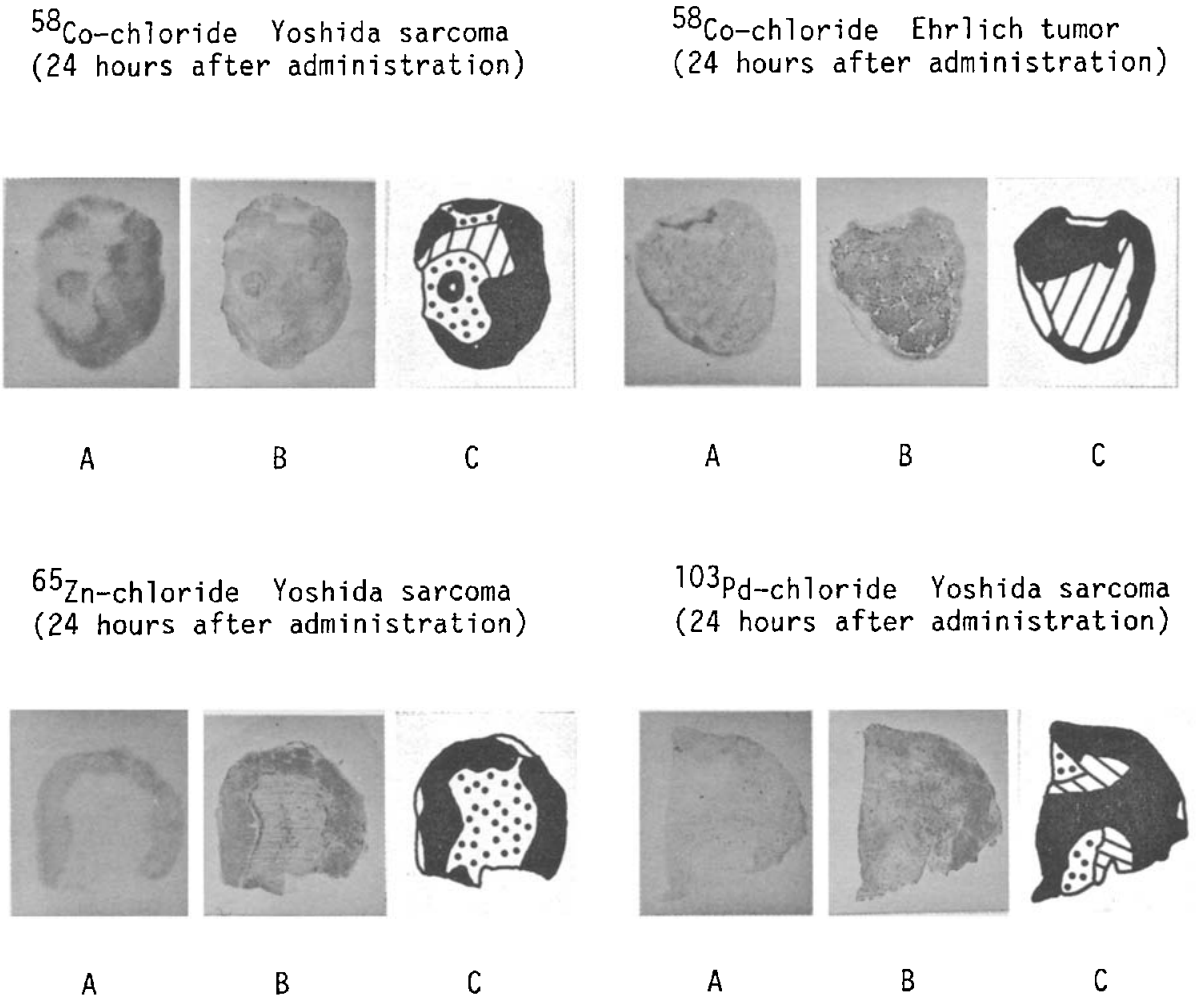

Figure 1. Morphological specimens: (**A**) macroautoradiogram; (**B**) hematoxylin–eosin staining; (**C**) sketch illustration. ■, Viable tumor tissue; ▨, tissue containing viable and necrotic tumor tissue; ⁙, necrotic tumor tissue; □, connective tissue (containing inflammatory tissue).

Distribution in tumor tissue

Hematoxylin–eosin-stained sections were classified into the following four categories: (i) viable tumor tissue, (ii) tissue containing viable and necrotic tumor tissue, (iii) necrotic tumor tissue, and (iv) connective tissue which contains inflammatory tissue. The distribution of these four groups is indicated in the sketch illustration in Figure 1. A typical autoradiogram of an Ehrlich tumor or Yoshida sarcoma of each nuclide is illustrated in Figure 1. In the case of animals injected with $^{65}ZnCl_2$, ^{65}Zn was concentrated in the viable tumor tissue and was not seen in the necrotic tumor tissues, regardless of time after administration. In the case of animals injected with $^{58}CoCl_2$, the concentration of ^{58}Co was more dominant in the connective tissue (especially inflammatory tissue) than in the other three kinds of tissues, regardless of time after administration. The concentration of this nuclide in viable tumor tissue was more dominant than in necrotic tumor tissue, regardless of time after injection. However, there were some cases where the concentration of ^{58}Co in borderline areas between viable tumor tissue and necrotic tumor tissue was more dominant than in the other tissues. In the case of animals injected with $^{103}PdCl_2$, the concentration of this nuclide was more dominant in viable tumor tissue than in the other tissues and was not seen in necrotic tumor tissue, regardless of time after administration. In the case of animals injected with $^{85}SrCl_2$, a clear result was not obtained because of the low uptake of this nuclide in tumor tissue.

Subcellular distribution in tumor and liver

When radioactivities of the nuclear fraction, mitochondrial fraction, microsomal fraction and super-

natant fraction are expressed as A (c.p.m.), B (c.p.m.), C (c.p.m.) and D (c.p.m.), respectively, radioactivity (percentage) of the nuclear fraction can be calculated by the following formula:

$$\frac{A}{A+B+C+D} \times 100\,(\%).$$

Radioactivities of the mitochondrial fraction, microsomal fraction and supernatant fraction were calculated by substitution of A with B, C and D in the numerator. Radioactivities of each fraction of the three different tumor and liver samples are shown in Tables 2 and 3.

Radioactivity of each fraction of the three different tumor samples is shown in Table 2. In three different tumors of animals administered with $^{65}ZnCl_2$, most of the ^{65}Zn was localized in the supernatant fraction, and a small amount in the nuclear fraction, microsomal fraction and mitochondrial fraction (lysosome is contained in this fraction). These values were approximately constant regardless of time after administration. In three tumors of animals administered with $^{85}SrCl_2$, a large amount of ^{85}Sr was localized in the supernatant fraction, and a small amount in the nuclear, mitochondrial and microsomal fractions. These values were approximately constant regardless of time after administration. Concerning the subcellular distribution of $^{58}CoCl_2$ in the three tumors, most of the ^{58}Co was localized in the supernatant fraction, but this nuclide decreased with time after administration. The ^{58}Co in the mitochondrial fraction of Yoshida sarcoma and hepatoma AH109A, and the ^{58}Co in the microsomal fraction and Yoshida sarcoma obviously increased with time after administration. In the case of $^{103}PdCl_2$, most of the ^{103}Pd was localized in the supernatant fraction and only a small amount in the other fractions. These values were approximately constant regardless of time after administration except for at 10 min.

The radioactivity of each fraction of liver samples is shown in Table 3. In liver of animals administered with $^{65}ZnCl_2$, most of the ^{65}Zn was localized in the supernatant fraction and only a small amount in the other fractions. These values were approximately constant regardless of time after administration. In the case of $^{85}SrCl_2$, quite a large amount of ^{85}Sr was localized in both the nuclear and mitochondrial fractions. The amount of this nuclide in the microsomal fraction was small and that in the supernatant was very small. These values hardly changed with time. In the case of ^{58}Co, the concentrations for the nuclear and mitochondrial fractions increased with time, and quite a large amount of this nuclide had accumulated in these fractions at 48 h after administration. Conversely this nuclide in the supernatant fraction decreased with time. The concentrations of ^{103}Pd in each fraction were relatively uniform and hardly changed with time.

Discussion

Retention values of ^{65}Zn for tumors were larger than for the other three nuclides. However, the values of ^{65}Zn for tumors are similar to those of ^{67}Ga, which is widely used to detect tumor lesions (Ando *et al.* 1985). Generally speaking, retention values of these bipositive metal ions were smaller than those of metal ions described above (Ando *et al.* 1982, 1983, 1985, 1987b; Ando & Ando 1986, 1990).

Concerning the accumulation of ^{67}Ga in tumor and normal tissues, Swartzendruber *et al.* (1971), using electron microscope autoradiography (EM-ARG), have shown that intracellular ^{67}Ga present in normal and neoplastic tissue is localized in lysosome-like bodies 1–2 days after intravenous administration in a variety of cell types. The subcellular fractionation and enzymatic studies reported by Brown *et al.* (1973, 1976) provided further evidence for the lysosomal nature of the organelles previously identified by EM-ARG. Takeda *et al.* (1977, 1978) showed lysosomal accumulation of ^{67}Ga and ^{111}In in the experimental tumor and liver. In contrast to the results described above, Deckner *et al.* (1971) on Ehrlich ascites cell, Orii (1972) on Yoshida sarcoma and Ito *et al.* (1971) on VX-2 carcinoma have indicated that little or no ^{67}Ga is associated with lysosomes in tumor tissues. On the basis of these reports, we investigated in detail the lysosomal role in the accumulation of radioactive metal ions in tumor and organs.

To date we have reported as follows: large amounts of ^{67}Ga (Ando *et al.* 1985), ^{111}In, ^{169}Yb (Ando *et al.* 1982), ^{167}Tm (Ando *et al.* 1983), ^{46}Sc, ^{51}Cr (Ando *et al.* 1987b), ^{95}Zr, ^{181}Hf (Ando & Ando 1986), ^{95}Nb and ^{182}Ta (Ando & Ando 1990) are concentrated in the mitochondrial fraction (containing lysosome) of liver, and lysosomes play an important role in the liver concentration of these nuclides. Quite large amounts of ^{46}Sc, ^{51}Cr, ^{95}Zr, ^{181}Hf, ^{95}Nb and ^{182}Ta are concentrated in the mitochondrial fraction (containing lysosome) of Yoshida sarcoma and Ehrlich tumor, but ^{67}Ga, ^{111}In, ^{169}Yb and ^{167}Tm are not concentrated in the mitochondrial fraction of these tumors. Lysosome plays a considerably important role in the tumor accumulation of ^{46}Sc, ^{51}Cr, ^{95}Zr, ^{181}Hf, ^{95}Nb and ^{182}Ta, but plays almost no role in the tumor

Table 2. Subcellular distribution (%) of radioactive bipositive metal ions in experimental tumors

	$^{65}ZnCl_2$					$^{85}SrCl_2$					$^{58}CoCl_2$					$^{103}PdCl_2$				
	10 min	60 min	3 h	24 h	48 h	10 min	60 min	3 h	24 h	48 h	10 min	60 min	3 h	24 h	48 h	10 min	60 min	3 h	24 h	48 h
Ehrlich tumor																				
nuclear fraction	16.1	12.4	13.8	15.6	14.4	16.4	15.6	14.4	20.1	21.3	4.9	5.3	12.8	13.6	15.3	1.4	20.3	13.9	19.4	20.4
mitochondrial fraction	8.1	4.8	5.3	7.0	5.3	9.3	12.4	9.9	13.7	12.1	5.5	7.7	9.0	10.5	14.1	0.5	19.5	18.5	18.3	20.7
microsomal fraction	15.7	12.7	12.1	20.3	19.5	19.3	18.7	20.2	17.4	18.3	7.8	6.6	9.8	10.9	13.0	21.2	8.5	9.2	12.0	11.9
supernatant fraction	60.1	70.1	68.8	57.1	60.8	55.0	53.3	55.5	48.8	48.3	81.8	80.4	68.4	65.0	57.6	76.9	51.7	58.4	50.3	47.0
Yoshida sarcoma																				
nuclear fraction	13.5	14.6	13.0	10.0	10.9	9.2	11.8	10.6	10.8	13.5	6.2	5.3	6.7	8.6	10.8	14.5	12.8	13.3	17.1	18.6
mitochondrial fraction	8.5	10.5	11.8	7.0	7.3	17.0	24.0	23.8	19.0	18.6	8.9	9.9	10.9	18.2	23.5	28.8	26.9	29.0	23.8	22.2
microsomal fraction	18.4	15.4	16.3	22.7	24.3	20.8	20.9	22.0	21.4	15.6	9.2	9.7	12.1	15.8	19.6	20.9	22.8	23.1	13.2	11.4
supernatant fraction	59.6	59.5	58.9	60.3	57.5	53.0	43.3	43.6	48.8	52.3	75.7	75.1	70.3	57.4	46.1	35.8	37.5	34.6	45.9	47.8
Hepatoma AH109A																				
nuclear fraction	15.5	18.3	15.7	15.4	17.9	18.0	14.4	22.1	23.3	24.3	6.8	10.2	9.1	14.0	13.3	18.0	20.1	18.2	21.0	16.9
mitochondrial fraction	6.7	5.1	5.1	8.0	6.3	15.1	17.3	23.5	20.3	20.2	6.4	7.8	8.7	17.0	20.8	19.7	23.1	20.9	22.0	23.7
microsomal fraction	15.2	15.0	20.2	20.2	21.3	24.5	23.7	22.4	20.8	19.2	8.1	7.0	9.6	12.5	10.8	23.0	20.9	14.8	18.5	14.1
supernatant fraction	62.6	61.6	59.0	56.4	54.5	42.4	44.6	32.0	35.6	36.3	78.7	75.0	72.6	56.5	55.1	39.3	35.9	46.1	38.5	45.9

Each value is expressed as a mean of three experiments.

Table 3. Subcellular distribution (%) of radioactive bipositive metal ions in rats and mice liver

	$^{65}ZnCl_2$					$^{85}SrCl_2$					$^{58}CoCl_2$					$^{103}PdCl_2$				
	10 min	60 min	3 h	24 h	48 h	10 min	60 min	3 h	24 h	48 h	10 min	60 min	3 h	24 h	48 h	10 min	60 min	3 h	24 h	48 h
Liver of mice with transplanted Ehrlich tumor																				
nuclear fraction	14.0	11.8	13.6	11.8	15.3	30.5	34.0	30.4	31.0	34.2	14.5	17.8	20.2	29.0	36.7	23.7	17.1	22.8	22.6	21.3
mitochondrial fraction	8.0	6.2	6.9	9.3	9.3	36.0	44.5	40.0	43.3	38.8	15.2	19.2	24.2	26.5	31.2	20.1	33.0	33.6	31.1	31.9
microsomal fraction	14.4	12.9	11.9	15.4	12.3	19.9	17.4	17.4	16.8	16.5	20.1	18.8	19.2	22.2	19.7	29.5	26.5	21.1	26.5	24.5
supernatant fraction	63.6	69.1	67.6	63.5	63.1	13.6	4.1	12.2	8.9	10.5	50.2	44.2	36.4	22.3	12.4	26.7	23.4	22.5	20.0	22.3
Liver of rats with transplanted Yoshida sarcoma																				
nuclear fraction	14.5	11.5	13.0	11.5	10.4	39.6	38.7	39.1	37.1	40.1	11.8	15.9	21.4	23.9	23.9	28.8	25.6	38.5	31.7	28.6
mitochondrial fraction	8.2	6.4	6.6	7.6	7.9	39.2	41.9	42.2	39.3	36.7	15.4	21.7	21.7	30.2	36.2	24.5	27.5	24.3	33.2	27.9
microsomal fraction	16.4	11.8	11.5	11.5	9.8	16.3	15.0	14.9	14.4	16.0	15.5	14.4	14.4	18.4	14.3	28.2	29.2	17.1	12.7	19.6
supernatant fraction	60.9	70.3	68.9	69.4	71.9	4.9	4.4	3.8	9.2	7.2	57.3	48.0	42.5	27.5	25.6	18.5	17.7	20.1	22.4	23.9
Liver of rats with transplanted Hepatoma AH109A																				
nuclear fraction	15.3	15.7	14.8	10.9	11.1	37.7	36.5	42.9	36.9	44.9	16.5	23.0	24.5	30.8	33.8	19.7	27.6	30.1	22.1	22.8
mitochondrial fraction	8.1	7.1	6.2	7.5	6.7	40.0	37.2	39.2	42.6	36.9	10.7	12.6	19.3	34.8	39.2	28.7	29.8	30.8	27.0	30.7
microsomal fraction	15.1	16.6	14.9	12.4	14.1	18.9	18.0	11.2	13.3	12.1	14.4	13.6	13.8	17.4	10.4	29.8	19.0	16.4	26.3	25.6
supernatant fraction	61.5	60.6	64.1	69.2	68.1	3.4	8.3	6.7	7.2	6.1	58.4	50.8	42.4	17.0	16.6	21.8	23.6	22.7	24.6	20.9

Each value is expressed as a mean of three experiments.

accumulation of ^{67}Ga, ^{111}In, ^{169}Yb and ^{167}Tm. Most of the alkaline metals and ^{201}Tl are in the supernatant fraction of tumor and liver (Ando *et al.* 1987a, 1988).

Subcellular distributions of ^{58}Co in liver and tumors were quite similar to those of ^{46}Sc, ^{51}Cr, ^{95}Zr, ^{181}Hf, ^{95}Nb and ^{182}Ta, and the distributions of ^{65}Zn were similar to those of alkaline metals and ^{201}Tl. Subcellular distributions of ^{85}Sr and ^{103}Pd were very different from the distributions of the above described nuclides. It has been clarified from our experiments that lysosome plays a fairly important role in the liver accumulation of ^{58}Co and plays a slight role in tumor accumulation of this nuclide.

Concerning the behavior of bipositive metal ions in tumor tissues, the distribution for ^{58}Co was very different from that of ^{65}Zn and ^{103}Pd. Regarding the distribution in tumor tissue and liver, ^{58}Co was fairly similar to ^{67}Ga, ^{111}In, ^{169}Yb, ^{46}Sc, ^{51}Cr, ^{95}Zr, ^{181}Hf, ^{95}Nb and ^{182}Ta.

^{65}Zn and ^{103}Pd were concentrated in viable tumor tissue and were not seen in the other three kinds of tissues. Considering the similarity of ^{65}Zn, ^{103}Pd and radioactive alkaline metals (Ando *et al.* 1988) (except for ^{22}Na) in tumor tissues, ^{65}Zn and ^{103}Pd might be taken up into the tumor cells.

References

Ando A, Ando I, Hiraki T, Takeshita M, Hisada K. 1982 Mechanism of tumor and liver concentration of ^{111}In and ^{169}Yb; ^{111}In and ^{169}Yb binding substances in tumor tissues and liver. *Eur J Nucl Med* **7**, 298–303.

Ando A, Ando I, Sakamoto K, Hiraki T, Hisada K, Takeshita M. 1983 Affinity of ^{167}Tm-citrate for tumor and liver tissue. *Eur J Nucl Med* **8**, 440–446.

Ando A, Ando I, Sanada S, *et al.* 1984 Study of the distribution of tumor affinity metal compounds and alkaline metal compounds in the tumor tissues by macroautoradiography. *Int J Nucl Med Biol* **11**, 195–201.

Ando A, Ando I, Sanada S, Hiraki T, Hisada K. 1985 Tumor and liver uptake models of ^{67}Ga-citrate. *Eur J Nucl Med* **10**, 262–268.

Ando A, Ando I. 1986 Distribution of ^{95}Zr and ^{181}Hf in tumor-bearing animals and mechanism for accumulation in tumor and liver. *Nucl Med Biol Int J Radiat Appl Instrum Part B* **13**, 21–29.

Ando A, Ando I, Katayama M, *et al.* 1987a Biodistributions of ^{201}Tl in tumor bearing animals and inflammatory lesion induced animals. *Eur J Nucl Med* **12**, 567–572.

Ando A, Ando I, Yamada N, Hiraki T, Hisada K. 1987b Distribution of ^{46}Sc and ^{51}Cr in tumor-bearing animals and the mechanism for accumulation in tumor and liver. *Nucl Med Biol Int J Radiat Appl Instrum Part B* **14**, 143–151.

Ando A, Ando I, Katayama M, *et al.* 1988 Biodistributions of radioactive alkaline metals in tumor bearing animals: comparison with ^{201}Tl. *Eur J Nucl Med* **14**, 352–357.

Ando A, Ando I. 1990 Distribution of ^{95}Nb and ^{182}Ta in tumor-bearing animals and mechanism for accumulation in tumor and liver. *J Radiat Res* **31**, 97–109.

Brown DH, Swartzendruber DC, Carlton JE, Byrd BL, Hayes RL. 1973 The isolation and characterization of gallium-binding granules from soft tissue tumors. *Cancer Res* **33**, 2063–2066.

Brown DH, Byrd BL, Carlton JE, Swartzendruber DC, Hayes RL. 1976 A quantitative study of the subcellular localization of ^{67}Ga. *Cancer Res* **36**, 956–963.

Deckner K, Becker G, Langowski U, Schwering H, Hornung G, Schnidt CG. 1971 Die subcelluläre Bindung von 67-Gallium in Ascites-Tumorzellen. *Z Krebsforsch* **76**, 293–298.

Hogeboom GH. 1955 Fractionation of cell components of animal tissues. In: Colowick SP. Koplan NO, eds. *Methods in Enzymology*, Vol. 1. New York: Academic Press; 16–19.

Ito Y, Okuyama S, Sato K, Takahashi K, Sato T, Kanno I. 1971 ^{67}Ga tumor scanning and its mechanisms studied in rabbits. *Radiology* **100**, 357–362.

Orii H. 1972 Tumor scanning with gallium (^{67}Ga) and its mechanism studied in rats. *Strahlentherapie* **144**, 192–200.

Swartzendruber DC, Nelson B, Hayes RL. 1971 Gallium-67 localization in lysosomal-like granules of leukemic and nonleukemic murine tissues. *J Natl Cancer Inst* **46**, 941–952.

Takeda S, Uchida T, Matsuzawa T. 1977 A comparative study on lysosomal accumulation of gallium-67 and indium-111 in Morris hepatoma 7316A. *J Nucl Med* **18**, 835–839.

Takeda S, Okuyama S, Takusagawa K, Matsuzawa T. 1978 Lysosomal accumulation of gallium-67 in Morris hepatoma-7316A and Shionogi mammary carcinoma-115. *Gann* **69**, 267–271.